Leaf anatomy does not explain apparent short-term responses of mesophyll conductance to light and CO_2 in tobacco

Marc Carriquí[a,†,*], Cyril Douthe[a,†], Arántzazu Molins[b] and Jaume Flexas[a]

[a]Research Group on Plant Biology under Mediterranean Conditions, Departament de Biologia, Universitat de les Illes Balears - Instituto de investigaciones Agroambientales y de la Economía del Agua (INAGEA), Palma, Illes Balears 07122, Spain

[b]Dpto. Botánica, ICBIBE & Jardí Botànic, Fac. CC. Biológicas, Universitat de València, C/ Dr. Moliner 50, 46100-Burjassot, Valencia, Spain

[†]These authors contributed equally to this work.

Correspondence

*Corresponding author,

e-mail: m.carriqui@uib.cat

Mesophyll conductance to CO_2 (g_m), a key photosynthetic trait, is strongly constrained by leaf anatomy. Leaf anatomical parameters such as cell wall thickness and chloroplast area exposed to the mesophyll intercellular airspace have been demonstrated to determine g_m in species with diverging phylogeny, leaf structure and ontogeny. However, the potential implication of leaf anatomy, especially chloroplast movement, on the short-term response of g_m to rapid changes (i.e. seconds to minutes) under different environmental conditions (CO_2, light or temperature) has not been examined. The aim of this study was to determine whether the observed rapid variations of g_m in response to variations of light and CO_2 could be explained by changes in any leaf anatomical arrangements. When compared to high light and ambient CO_2, the values of g_m estimated by chlorophyll fluorescence decreased under high CO_2 and increased at low CO_2, while it decreased with decreasing light. Nevertheless, no changes in anatomical parameters, including chloroplast distribution, were found. Hence, the g_m estimated by analytical models based on anatomical parameters was constant under varying light and CO_2. Considering this discrepancy between anatomy and chlorophyll fluorescence estimates, it is concluded that apparent fast g_m variations should be due to artifacts in its estimation and/or to changes in the biochemical components acting on diffusional properties of the leaf (e.g. aquaporins and carbonic anhydrase).

This article has been accepted for publication and undergone full peer review but has not been through the copyediting, typesetting, pagination and proofreading process, which may lead to differences between this version and the Version of Record. Please cite this article as doi: 10.1111/ppl.12755

Abbreviations – A, net photosynthesis; C_c, chloroplast CO_2 concentration; C_i, substomatal CO_2 concentration; ETR, electron transport rate; f_{ias}, fraction of intercellular air spaces; g_m, mesophyll conductance; $g_{m,\ anat}$, mesophyll conductance inferred by anatomy measurements; g_s, stomatal conductance; J_{max}, maximum electron transport rate; L_{chl}, chloroplast length; l_{ias}, gas phase limitations to photosynthesis; l_i, liquid phase limitations to photosynthesis; LMA, leaf mass area; p_{cw}, cell wall porosity; R_d, non-photorespiratory CO_2 release -respiration- in the light; S_c/S, chloroplast surface area exposed to intercellular air spaces per unit of leaf area; S_m/S, mesophyll surface area exposed to intercellular air spaces per unit of leaf area; T_{chl}, chloroplast thickness; T_{cw}, cell wall thickness; T_{cyt}, cytoplasm thickness; T_{leaf}, leaf thickness; T_{mes}, mesophyll thickness; $V_{c,max}$, maximum velocity of carboxylation.

Introduction

The rates of photosynthesis in vascular plants depend on the stomatal conductance (g_s), the mesophyll conductance to CO_2 (g_m) and the biochemical capacity to fix carbon. Mesophyll conductance has been widely estimated for hundreds of species, and its response to environmental changes (i.e. light, CO_2, temperature) has been reported. Two methods are the most widely recognised and used to assess g_m variations, the stable isotope method based on the discrimination of ^{13}C during photosynthesis (Evans 1989, Lloyd et al. 1992), and the variable J method based on leaf chlorophyll fluorescence (Harley et al. 1992). Both methods have revealed that g_m is finite and largely varying in response to environmental conditions, both in the short and long term, depending on the species and conditions (Flexas et al. 2012, Griffiths and Helliker 2013). However, the basics of g_m and its regulation are not fully understood, arising a continuous scientific debate. One of the major current controversies on g_m is whether the dynamic response of g_m to fast environmental changes (i.e. during a typical A-PAR or A-C_i curve) is real, apparent or even artifactual. On the one hand, g_m has been found to vary rapidly (within minutes) with changes in [CO_2] (Douthe et al. 2011, 2012, Flexas et al. 2007b, Hassiotou et al. 2009, Xiong et al. 2015, Yin et al. 2009), light (Douthe et al. 2011, 2012, Hassiotou et al. 2009, Xiong et al. 2015), or temperature (von Caemmerer and Evans 2015, Yamori et al. 2006). On the other hand, some studies did not found those rapid changes under light or CO_2 (Tazoe et al. 2009).

Assuming the observed fast changes of g_m are real, they should reflect a physiological process, which could be explained by at least two mechanisms. The first mechanism would imply that at least one of the anatomical resistances change, in seconds or minutes, significantly enough to modify g_m. The path for CO_2 starts from air-diffusion from the sub-stomatal cavity to the mesophyll cells, where it dissolves and continues by aqueous diffusion through the cell wall, plasma membrane, cytosol and chloroplast envelope. The two main anatomical determinants of g_m are the cell wall thickness (T_{cw}) and the chloroplast surface area exposed to the intercellular air spaces (S_c/S) (Evans et al. 2009, Tomás et al. 2013, Tosens et al. 2016). The estimation of anatomical parameters allowed the establishment of a simplified 1-D anatomical model of diffusion (a steady-state model) that gave estimations of g_m very close to those estimation from gas exchange (Peguero-Pina et al. 2017, Tomás et al. 2013, Tosens et al. 2012, 2016, Veromann-Jürgenson et al. 2017, Xiao and Zhu 2017), but potential rapid changes in anatomical arrangements in response to light or CO_2 have not been experimentally tested. The second mechanism implies that biochemical factors change resistances in the CO_2 pathway through the mesophyll. Such mechanism could be related with the diffusion facilitation provided by aquaporins across the plasma membrane and possibly chloroplast membrane (Flexas and Diaz-Espejo 2015, Heinen et al. 2009, Perez-Martin et al. 2014, Uehlein et al. 2008) and by carbonic anhydrase in the cytosol (Ho et al. 2016, Momayyezi and Guy 2017, Tholen and Zhu 2011).

Focusing on the first potential mechanism, most of the anatomical limitations are considered invariable in the short term (Evans et al. 2009, Terashima et al. 2011). Indeed, it is difficult to imagine large enough changes in the cell wall composition in minutes to cause the observed changes in g_m. Thus, the main candidate to explain the observed rapid g_m changes from an anatomical point of view would be the movement of chloroplasts, which could induce changes in S_c/S (Oguchi et al. 2005, Tholen et al. 2008). Tholen et al. (2008) observed in *A. thaliana* that a short-term increase of blue light intensities produced a reduction of S_c/S to avoid photodamage, which resulted in changes of g_m as measured by the online ^{13}C method. Similarly, transferring sun plants from low to high growth irradiance, Oguchi et al. (2005) described in leaves of deciduous species an increase of S_c/S provoked by the movement of the chloroplast towards intercellular airspaces, that was linked with an increase of photosynthesis. Species-dependent behaviour can be the cause of such apparent discrepancies, highlighting the need of further studies in this topic (Higa and Wada 2016, Ho et al. 2016, Théroux-Rancourt and Gilbert 2017). Moreover, to date there is no direct measurement of the potential change of chloroplast surface area exposed to intercellular airspace during an *A*-PAR or *A*-Ci curve, which would help to elucidate this debate.

If anatomy cannot explain apparent the fast variations of g_m, there are two options remaining: (1) either biochemical factors modifying g_m without any anatomical changes, or (2) apparent g_m variations do not reflect a “true” biological process. The latter may be originated by a “mathematical artifact” and/or by an “over-simplification” of the model used. Mathematical dependencies of the output (here g_m) on the values of other variables (mainly *A* and C_i) used to compute it, can provoke “artifactuals” estimates (Gu and Sun 2014). Indeed, the shape of the equations used (Harley et al. 1992, Lloyd et al. 1992) can produce a systematic relationship between *A* or C_i and g_m (and any other variable that can vary with them, including light), producing erroneous g_m estimates. The use of wrong values of Γ^* and/or R_d can also produce such artifact (an obligatory relationship between g_m and C_i, for example). Secondly, wrong estimates can be obtained by “over-simplification”, i.e. when the hypothesis of the model behind is wrong, or are too simplified when compared to “reality”. For example, Tholen and

Zhu (2011) claimed that the possibility of CO_2 recycling during photosynthesis, especially under low light/CO_2, would affect apparent g_m estimates and should be taken into account, as well as the importance of the resistance of the chloroplast membrane. In this case, 3D modelling could help to take into account position and number of mitochondria and the subsequent CO_2 fluxes between chloroplast and mitochondria (Xiao and Zhu 2017). Later, Yin and Struik (2017) proposed a generalised model including/improving the claims of Tholen and Zhu (2011), adding new parameters to the model to reflect the mitochondrial positioning in respect to the chloroplast membrane. The light gradient through the leaf profile has also been identified as a key parameter that strongly influences photosynthesis efficiency (Evans and Vogelmann 2003, Terashima and Saeki 1985, Vogelmann et al. 1989). Those light gradients through the leaf profile are also likely to produce distinct contributions of each layer to the mesophyll, producing apparent (i.e. not reflecting the "true" biological) variations of g_m at different measuring lights (Evans 2009, Théroux-Rancourt and Gilbert 2017). Several recent studies also focused on light gradients or integrate the influence of photorespired CO_2 in a generalized model for g_m. Nevertheless, up to present, the proposed models are either based on a theoretical approach alone, or they contain numerous parameters that are difficult to estimate.

The aim of this study is to experimentally test whether the observed fast changes of g_m in a typical *A*-PAR or *A*-C_i curve could be totally or partially due to anatomical changes. Furthermore, the relationship between g_m values estimated by either the fluorescence or by two analytical models based on anatomical parameters was also investigated.

Materials and methods

Seeds of tobacco (*Nicotiana tabacum* L.) were sowed and germinated in a tray with horticultural substrate and placed in a growth chamber with a 12/12h light/dark regime and temperature fixed at 25/20ºC day/night. Seedlings were watered every two days. After 2 weeks, seedlings were transferred in 4-l pots containing organic soil and perlite (75:25 by vol.). Plants were grown under low to moderate light intensity at plant height for this species (Flexas et al. 2006, Galle et al. 2009, Galmés et al. 2006), 300 µmol m^{-2} s^{-1} PPFD (1000W HPS lamps, OSRAM), and maintained under optimal water conditions, watered with 25% Hoagland's solution twice a week. Growing light intensity was chosen, on the one hand, to avoid a possible loss of functionality of the chloroplast avoidance movement, as observed by Higa and Wada (2016) in leaves of climbing plants grown under strong light. On the other hand, the objective was to obtain a leaf mass per area (LMA) in the lower range of reported values in bibliography for this species (Flexas et al. 2006). Lower LMA implies lower leaf thickness and simpler mesophyll structure (Poorter et al. 2009), minimizing the potential bias between chlorophyll fluorescence with gas exchange caused by contrasting photosynthetic contribution of different cell layers (Evans 2009, Théroux-Rancourt and Gilbert 2017) and/or by blue light absorption close to the illuminated surface (Brodersen and Vogelmann 2010, Evans and Vogelmann 2003). Measuring light intensities (200, 600 and 1500 µmol m^{-2} s^{-1}) were chosen to respond to two constraints: we could not use too extreme low light, because it could produce unreliable values of g_m, while the high light treatment should be far enough to induce chloroplast movements if these were a response to varying CO_2. Measurements were performed in 40-50 days old plants. All measurements were performed on the first or second youngest fully expanded leaf to ensure mature leaf anatomy and to avoid age variations between the plants.

Gas exchange and chlorophyll fluorescence measurement

Leaf gas exchange parameters were measured using a portable photosynthesis system (Li-6400; Li-Cor, Inc., Nebraska, USA) with an infrared gas analyser (IRGA) coupled with a 2 cm^2 leaf fluorescence chamber (Li -6400-40 leaf chamber fluorometer; Li-Cor, Inc.) All measurements were carried out between 09:00 and 19:00 h (Central European summer time). Block temperature was fixed at 25ºC, air flow rate at 300 µmol min^{-1} and VPD kept around 1.5 kPa for all measurements.

Leaves from randomly selected plants were fully characterized. Leaf steady-state conditions were induced at 400 µmol CO_2 mol^{-1} air and saturating photosynthetic photon flux density (PPFD 1500 µmol m^{-2} s^{-1}, 90:10 red:blue light). Once steady state conditions were achieved, always after 15-20 minutes, complete light and CO_2 response curves at 21 and 2% O_2 were performed in a random order. Light response curves were measured at 400 µmol CO_2 mol^{-1} air at PPFD of 2000, 1500, 1000, 800, 600, 400, 200, 150, 100, 50 and 0 µmol m^{-2} s^{-1}. CO_2 response curves were measured at PPFD 1500 µmol m^{-2} s^{-1} at cuvette CO_2 concentration (C_a) of 400, 300, 200, 150, 100, 50, 0, 400, 400, 600, 800, 1000, 1200, 1500 and 2000 µmol mol^{-1}. Four to five curves were performed per response curve type. The order in which curves were performed did not affect the responses (data not shown). Non-photorespiratory respiration during the day (R_d) was estimated by dividing by 2 the respiration rate measured after 2 h of darkness (Martins et al. 2013, Niinemets et al. 2005, Veromann-Jürgenson et al. 2017). Any measurement performed at a non-ambient [CO_2] was corrected for leaks following Flexas et al. (2007a).

Once homogeneous responses among plants at the same conditions were verified with both light and CO_2 response curves, leaves from randomly selected plants were short-term acclimated (10-15 minutes) to a specific light and CO_2 treatment. Five treatments were applied, consisting of three light intensities, low, moderated and saturating, and ambient C_a, and low and high C_a at saturating light (see Table 1 for each conditions applied). After the acclimation period, five logs were recorded at approximately 1 min interval. Directly after measurements, the exact portion of leaf that was inside the Li-6400-40 chamber was sampled and instantaneously (below 30 s) cut into small pieces after immersion under fixator for subsequent anatomical measurements. This procedure was repeated on 6 to 8 different plants per treatment.

Values of A and steady-state fluorescence (F_s) were registered just after the steady-state conditions for gas exchange were achieved. Then a saturating white light flash around 8000 µmol m^{-2} s^{-1} was applied to determine the maximum fluorescence (F_m'). Multiphase flash methodology for chlorophyll fluorescence measurements was followed, as suggested by Loriaux et al. (2013), to avoid potential maximum yield underestimation error. The electron transports rate (ETR) was estimated from Genty et al. (1989) as ETR = PPFD × ΦPSII × α × β, being ΦPSII the efficiency of photo-system II, α the leaf absorbance and β the electrons partitioning between photo-systems I and II. ΦPSII was estimated as ΦPSII = (F_m'-F_s)/F_m' (Genty et al. 1989). The α·β parameter was estimated following (Valentini et al. 1995). CO_2 response curves under non-photorespiratory conditions in a low O_2 atmosphere (< 2%) were performed in order to establish the relationship between ΦPSII and ΦCO_2 under non-photorespiratory conditions (with ΦCO_2 = (A + R_d)/PPFD), then considering α × β = 4/b where b is the slope of the ΦPSII ~ ΦCO_2 relationship. We obtained α × β = 0.44. Then, g_m was estimated following Harley et al. (1992), as:

$$(1)\quad g_m = \frac{A}{C_i - \frac{\Gamma^*(ETR + p2(A+R_d))}{(ETR - p1(A+R_d))}}$$

where A is the net assimilation rate, Γ* is CO_2 compensation point in absence of R_d, and C_i the CO_2 concentration in intercellular air-spaces. Γ* was assumed to be 40 µmol mol^{-1} in *N. tabacum* as in Walker et al. (2013). Values of $p1$ and $p2$ depend on the limited steps of RuBP regeneration. In this study we assumed that RuBP regeneration is limited by NADPH, so p_1 = 4 and p_2 = 8, but another two combinations were used in a sensitivity analysis (p_1 = 4 and p_2 = 9.33 and p_1 = 4.5 and p_2 = 10.5) for ATP limited regeneration (Gu and Sun 2014). After calculation, g_m data were filtered following the reliability criterion established by Harley et al. (1992), in which only data with values of dC_c/dA_N between 10 and 50 can be considered as reliable. Moreover, in order to try to get an improved estimate of g_m, the method proposed by Yin et al. (2009) was tested, as:

$$(2)\quad A = 0.5\left\{\frac{J}{4} - R_d + g_m(C_i + 2\Gamma_*) - \sqrt{\left[\frac{J}{4} - R_d + g_m(C_i + 2\Gamma_*)\right]^2 - 4g_m\left[(C_i - \Gamma_*)\frac{J}{4} - R_d(C_i + 2\Gamma_*)\right]}\right\}$$

and

(3) $A = \frac{C_i - \frac{A}{g_m} - \Gamma_*}{4(C_i - \frac{A}{g_m} + 2\Gamma_*)} - R_d$

In both cases of equation 2 and 3, g_m was solved with a solver in order to match the predicted *A* from Eq. 2 and 3 with the measured *A*.

Leaf mass per unit area

Leaf discs of known area were taken from measured leaves and placed in an oven at 60ºC until constant dry weight was reached to calculate the dry leaf mass per unit leaf area (LMA).

Anatomical measurements

Immediately after gas-exchange measurements, small leaf pieces (3 × 1 mm) of the area enclosed in the leaf chamber were cut off between the main veins per sample and immersed under the fixing solution. In order to prevent any anatomical change that may occur during cuts, when this process took more than 30 s the sample was discarded. Samples were quickly fixed with glutaraldehyde 4% and paraformaldehyde 2% in a 0.1 M phosphate buffer (pH 7.4) under vacuum pressure. Between 4 and 6 samples were taken per treatment. Afterwards, samples were post-fixed in 2% buffered osmium tetroxide for 2h, and dehydrated in a graded series of ethanol. Dehydrated samples were embedded in resin (LRwhite, London Resin Company, London, UK) and solidified in an oven at 60ºC for 48h.
Semi-thin cross-sections of 0.8 µm and ultrathin cross-sections of 90 nm for transmission electron microscopy (TEM) were cut with an ultramicrotome (Leica UC6, Vienna, Austria). Semi-thin sections were dyed with 1% toluidine blue and observed at 200× magnifications under an Olympus BX60 (Olympus, Tokyo, Japan) light microscopy and photographed with a Moticam 3 (Motic Electric Group Co., Xiamen, China). The ultrathin sections were contrasted with uranyl acetate and lead citrate and viewed at 1200× and 30000× magnifications with a transmission electron microscopy (TEM H600; Hitachi, Tokyo, Japan). All images were analysed using IMAGEJ software (Schneider et al. 2012). From light microscopy images leaf thickness (T_{leaf}), mesophyll thickness (T_{mes}), number of palisade layers and fraction of the mesophyll occupied by intercellular airspaces (f_{ias}) were measured. From TEM microscopy images cell wall thickness (T_{cw}), cytoplasm thickness (T_{cyt}), chloroplast length (L_{chl}), chloroplast thickness (T_{chl}) and mesophyll and chloroplast surface area exposed to intercellular airspace (S_m/S and S_c/S) were measured and calculated following Tomás et al. (2013). Cell curvature correction factor was calculated according to Thain (1983). Factors between 1.18 and 1.38 were applied to cell surface area estimates, depending on whether the measurement was performed in palisade (prolate spheroids) or spongy (oblate spheroids) mesophyll tissue. Four to six randomly selected different fields of view were considered per plant replicate to measure each anatomical characteristic. For each type of mesophyll tissue (spongy and palisade), ten measurements were made

for T_{leaf}, T_{mes}, f_{ias}, T_{cw}, S_m/S and S_c/S, and 15 measurements per mesophyll type were made for L_{chl} and T_{chl}. Then, weighted averages based on tissue volume fractions were calculated.

Estimation of mesophyll conductance modelled from anatomical characteristics

Analytical models for mesophyll conductance modelling of Niinemets and Reichstein (2003) and Xiao and Zhu (2017) were applied. The one-dimensional within-leaf gas diffusion model of Niinemets and Reichstein (2003) modified by Tomás et al. (2013) was applied. Mesophyll diffusion conductance as a composite conductance for within-leaf gas, liquid and lipid components is given as:

(4) $g_m = \frac{1}{\frac{1}{g_{ias}} + \frac{RT_k}{H \cdot g_{liq}}}$

where H is the Henry's law constant (m^3 mol^{-1} K^{-1}), R is the gas constant (Pa m^3 K^{-1} mol^{-1}) and T_k is the absolute temperature (K). $H/(RT_k)$ is the dimensionless form of Henry's law constant needed to convert a liquid and lipid phase conductance (g_{liq} and g_{lip}) into a gas-phase equivalent conductance (Niinemets and Reichstein 2003). Gas-phase diffusion depends on the fraction of mesophyll volume occupied by intercellular air spaces (f_{ias}, m^3 m^{-3},) and the effective diffusion path length in the gas-phase (ΔL_{ias}) (Syvertsen et al. 1995, Terashima et al. 2011):

(5) $g_{ias} = \frac{D_a \cdot f_{ias}}{\Delta L_{ias} \cdot \varsigma}$

where ς is the diffusion path tortuosity (m m^{-1}) and D_a (m^2 s^{-1}) is the diffusion coefficient for CO_2 in the gas-phase ($1.51 \cdot 10^{-5}$ m^2 s^{-1} at 22°C). ΔL_{ias} was approximated by mesophyll thickness divided by two (Niinemets and Reichstein 2003). An estimate of ς was used as a default value of 1.57 m m^{-1} (Niinemets and Reichstein 2003, Syvertsen et al. 1995). The total liquid phase conductance is provided by the sum of the inverse of serial conductances:

(6) $\frac{1}{g_{liq}} = \left(\frac{1}{g_{cw}} + \frac{1}{g_{pl}} + \frac{1}{g_{ct}} + \frac{1}{g_{en}} + \frac{1}{g_{st}}\right) \cdot S_c/S$

where partial conductances are for cell wall (g_{cw}), plasmalemma (g_{pl}), cytosol (g_{ct}), chloroplast envelope (g_{en}), and chloroplast stroma (g_{st}). The cell wall, cytosol and stromal conductances are given by a general equation:

(7) $g_i = \frac{r_{f,i} \cdot D_w \cdot p_i}{\Delta L_i}$

where g_i (m s^{-1}) is either g_{cw}, g_{ct} or g_{st}, ΔL_i (m) is the diffusion path length and p_i (m^3 m^{-3}) is the effective porosity in the given part of the diffusion pathway, D_w is the aqueous phase diffusion coefficient for CO_2 ($1.90 \cdot 10^{-9}$ m^2 s^{-1} at 22°C) and the dimensionless factor $r_{f,i}$ accounts for the decrease of diffusion conductance compared to free diffusion in water (Weisiger 1998). For cell walls where the aqueous-phase diffusion has been shown to approximate free water, $r_{f,i}$ = 1 (Rondeau-Mouro et al. 2008). The value of r_f was set at 0.3 for g_{ct} and g_{st} to account for the reduction of diffusion conductance due to high concentrations of high molecular solutes and intracellular (cytoskeleton) and intraorganellal (thylakoids) heterogeneities (Niinemets and Reichstein 2003). Effective porosity, p_i, was taken as 1 for g_{ct} and g_{st}. Cell wall porosity (p_{cw}) was taken as 0.1, as applied in (Tomás et al. 2014). Conductance in units of m s^{-1} can be converted into molar units considering that

$g[\text{mol m}^{-2} \text{ s}^{-1}] = g[\text{m s}^{-1}]44.6 \cdot [273.16/(273.16 + T_L)(P/101.325)$,

where T_L is the leaf temperature (ºC) and P (Pa) is the air pressure.

Due to the difficulty to measure the thickness of the plasma membrane, the chloroplast envelope and the limited information about the permeability of the lipid phase membranes, g_{pl} and g_{env} were assumed as constant values (0.0035 m s^{-1}) as previously suggested in other studies (Evans et al. 1994, Peguero-Pina et al. 2012, Tomás et al. 2013, Tosens et al. 2012a, 2012b).

The analytical model of Xiao and Zhu (2017) is based on the Niinemets and Reichstein (2003) model, considering besides the effect of CO_2 diffusion the process of hydration, biochemical parameters describing carbonic anhydrases (CA) and the environmental variables *A*, Ci, HCO_3^- leakage across the chloroplast envelope, the mitochondrial respiration and photorespiration rate and the relative position between chloroplasts and mitochondria. Assumed biophysical parameters for the diffusion properties of CO_2 in each subcellular resistance considered in the first analytical model were maintained when applying the Xiao and Zhu (2017) model. Other assumptions needed for the Xiao and Zhu (2017) model were used as in the cited paper. Unit conversions needed for fluxes conversion were applied as described in Methods S1. The relative position between mitochondria and chloroplasts could not be measured from ultrathin cross-section images, so a sensitivity analysis changing the fractionation factor for CO_2 (photo)respiration recycling from 0 to 1 was performed.

Statistical analysis

Independent one-way analysis of variance (ANOVA) was performed to check differences between treatments, for both light and CO_2 treatments. Differences between means were detected by Tukey's honest significant difference tests (with accepted $P < 0.05$). Pearson correlation matrices were determined for each group of treatments to determine the correlations between the different parameters. All analyses were performed with the R software (R Core Team 2016). Tukey's Post-Hoc tests were performed using the R "agricolae" package (Mendiburu 2015).

Results

Variation in photosynthetic parameters

Under ambient conditions (C_a 400 µmol CO_2 mol^{-1} air and PPFD 1500 µmol m^{-2} s^{-1}), plants showed net assimilation rate (*A*) of 16.7 µmol m^{-2} s^{-1}, stomatal conductance for water (g_s) of 0.28 mol m^{-2} s^{-1} and mesophyll conductance (g_m) of 0.14 mol m^{-2} s^{-1} (Fig. 1). *A*, g_s and g_m all decreased with decreasing light. This induced a slight decrease of C_i between low and high light treatments. In all cases, no differences were found between 1500 and 600 µmol m^{-2} s^{-1} PPFD, but differences were significant between 600 and 200 µmol m^{-2} s^{-1} PPFD (Fig. 1). When C_a was increased from ambient to 1500 µmol CO_2 mol^{-1} air, *A* significantly increased from 16.7 to 20.6 µmol m^{-2} s^{-1}, and both g_s and g_m decreased to 0.07 and 0.03 mol m^{-2} s^{-1}, respectively (Fig. 2). Statistical differences between the treatment at 100 µmol CO_2 mol^{-1} and the other two concentrations could not be proved, as only 1 data point for the low CO_2 passed the filtering of the Harley's criterion. Nevertheless, we observed that g_m data for 100 µmol CO_2 mol^{-1} were of the same range as at ambient CO_2, or even higher (Fig. S2). Statistical differences between g_m averages obtained for the different CO_2 and light treatments were corroborated by a sensitivity analysis performed for each variable needed for g_m estimation (Fig. S3). We also found the same range of values of g_m when estimated with the Yin et al. (2009) method (Fig. S4).

Variation in leaf anatomy and chloroplast arrangement

In order to identify any hypothetical change in the CO_2 pathway length from the substomatal cavity to the carboxylation site inside the chloroplast, a complete structural and ultrastructural analysis was performed of the photosynthetic organs in each short-term CO_2 and light variation. Little variability was observed in structural and ultrastructural parameters in response to CO_2 or light changes (Fig. S5 and Tables 1 and 2, respectively). LMA, which was not expected to change in the short-term range, was of 22 ± 2 g m^{-2}. Non-significant changes for most leaf anatomical parameters were found among CO_2 treatments (T_{leaf}, T_{mes}, number of palisade layers, f_{ias}, S_m/S, S_c/S, S_c/S_m, T_{cw}, T_{cyt} and L_{chl}; Table 2 and Fig. S5) except for chloroplast thickness (T_{chl}), which ranged from 2.81 ± 0.06 µm at 100 µmol CO_2 mol^{-1} air CO_2 to 3.44 ± 0.10 µm at 400 µmol CO_2 mol^{-1} air CO_2. Regarding to light treatments (Table 3 and Fig. S5), non-significant changes were observed in leaf anatomy except for chloroplast length (L_{chl}), which increased significantly from low light treatment (5.60 ± 0.22 µm) to high light treatments (and 6.28 ± 0.13 µm, respectively), although no significant differences were found between moderate light (5.70 ± 0.12 µm) and either low or high light treatments. No significant differences were found between light and CO_2 treatments for g_m as modelled from anatomy following Tomás et al. (2013; Tables 2 and 3). Consequently, no relationship was found between g_m modelled following Tomás et al. (2013) and g_m estimated following Harley et al. (1992; Figs 3A, 4). Considering S_c as the main determinant for g_m short-term variation, a theoretical fitting model revealed that S_c should vary between 0 and 12 m^2 m^{-2} in order to explain the observed short-term variation of g_m as estimated following Harley et al. (1992; Fig. 3A, B). If potential changes in plasma membrane conductance (g_{pl}) were considered as the main determinant of g_m short-term variation, g_{pl} should have varied between 0.00 and 0.14 mol m^{-2} s^{-1} (Fig. 3C, D). We can note that only the lower values of g_m were very close to the 1:1 relationship, the highest values were impossible to fit with Harley's method. Marginally significant correlation ($P < 0.1$) was obtained between g_m modelled following Xiao and Zhu (2017) and that estimated following Harley et al. (1992; Fig. 4). However, any weak correlation disappeared when partial or total CO_2 recycling from (photo)respiration was being considered (Fig. S7).

Discussion

Photosynthetic parameters and their response to CO_2 and light variations

Values of net assimilation rate and other photosynthetic traits were within the ranges usually described in the literature (Flexas et al. 2006, 2007b, Galle et al. 2009). The response of g_m observed in *Nicotiana tabacum* (Fig. S1) was the same as typically found in the literature for both CO_2 and light changes, with an expected curvilinear decrease with increasing C_i and an increase with increasing light (Figs 1 and 2). This fits well with the responses already described for different species, using either the Harley method or the isotope discrimination method (Flexas et al. 2008, Xiong et al. 2015, Yin et al. 2009, Hassiotou et al. 2009, Douthe et al. 2011, 2012). Usually, the apparent g_m response to light describes a curvilinear response, with a saturation plateau at high PPFD (Douthe et al. 2011, Yin et al. 2009). This could explain why no significant differences were found for g_m between 600 and 1500 µmol m^{-2} s^{-1}. When Harley and colleagues (1992) developed their model, they warned about g_m values measured at low or high [CO_2] and the possibility that they may not be reliable, providing a mathematical criterion to discern the reliability of the data. The application of this criterion to our data caused the removal of the vast majority of data measured at low C_i and some at high C_i. Nevertheless, it could be observed that those values were respecting the common pattern usually observed: g_m tends to increase at low C_i and is strongly decreased at $C_i > 1000$ µmol mol^{-1}. Altogether, the results confirm that a typical apparent [CO_2] and light g_m response described thus far was obtained.

Leaf anatomical parameters and the absence of response to CO_2 and light variations

No previous work has shown a detailed quantitative anatomical analysis in *N. tabacum*, although most of the parameters determined in the present study are within the expected range for non-sclerophyll, thin leaves (Tomás et al. 2013). Tobacco leaves, even after being subjected to short-term acclimation to different CO_2 and light treatments to induce fast changes in g_m, did not experienced significant changes in most anatomical parameters (Tables 2 and 3). Indeed, most of them have been suggested to be invariable in the short term (Evans et al. 2009, Terashima et al. 2011). The only significant change was observed in the chloroplast shape. Chloroplasts had lower thickness at low light and higher length at high CO_2 (Table 2). This could be associated to changes in chloroplast from the face to the profile position, as a chloroplast avoidance effect (Kasahara et al. 2002, Trojan and Gabrys 1996). Even so, it would be possible that during the time elapsed between taking the sample from the IRGA chamber and the fixation (below 30 s), any additional anatomical differences having possibly occurred could have been reversed. Despite these small changes in chloroplast arrangement between different treatments, chloroplast surface area exposed to intercellular air spaces per unit of leaf area (S_c) did not significantly change among light or CO_2 treatments.

Being S_c/S one of the major anatomical determinants of g_m (Evans et al. 2009, Peguero-Pina et al. 2017, Terashima et al. 2011, Tomás et al. 2013, Tosens et al. 2016), the extent of S_c/S variation that would independently explain the variation of g_m estimated via the Harley's method (Fig. 3A, B) was analyzed. The measured S_c/S was 6-8 m^2 m^{-2}, while it should have varied between 0 and 12 m^2 m^{-2} in order to obtain a modelled $g_{m,anatomy}$ similar to the variable g_m observed by the variable *J* method (Harley et al. 1992; Fig. 3A, B). A similar simulation was performed for plasma membrane conductance (g_{pl}), as plasma membrane aquaporins could potentially affect the g_m short-term variations by modifying g_{pl}. While for the $g_{m,anatomy}$ modelling, a constant value of 0.0035 m s^{-1} was assumed, g_{pl} should have varied between 0.00 and 0.14 m s^{-1} in order to bring closer anatomical and Harley's g_m (Fig. 3C, D). Even under these circumstances, the highest g_m values were still impossible to be fitted. In both cases, the huge range of variations needed for S_c/S and g_{pl} to fit Harley g_m seems unreliable in the short term. These results, based on measurements and simulations, tend to invalidate the possibility that fast changes of Harley's g_m observed in a typical *A*-PAR or *A*-C_i curve could be primarily associated to anatomical and/or aquaporin CO_2 diffusion changes in the CO_2 diffusion pathway through the mesophyll. Considering one of the recently published analytical models (Xiao and Zhu 2017), which incorporates to the 1-D diffusion model of Niinemets and Reichstein (2003) for g_m modelling additional variables such as measured gas exchange fluxes, (photo)respiration rates, carbonic anhydrase activities and HCO_3^- leakage, only a slight improvement was found when correlated with Harley et al. (1992). Marginal correlation (R^2 = 0.36) and far from the 1:1 relationship was obtained when considering both CO_2 and light treatments together but no (photo)respiration fractionation effect (Fig. 4). Considering partial or total fractionation of recycled CO_2 (e.g. considering different relative positions of mitochondria to chloroplasts) resulted in no correlation between both g_m estimates, suggesting that CO_2 recycling had minimal effect on g_m dynamic response in tobacco (Fig. S7).

Apparent discrepancy between gas exchange and leaf anatomy

Strong discrepancy between g_m estimated via the Harley's method and the estimations based on anatomy was observed (Fig. 4). These results contrast with the good agreement previously observed when comparing the two estimates among different species with contrasting leaf structure (Peguero-Pina et al. 2017, Tomás et al. 2013, Tosens et al. 2016, Veromann-Jürgenson et al. 2017) or comparing different leaf ontogenetic states within a species (Tosens et al. 2012). Apparently, this correlation falls down when applied to short-term variations, as observed in Tomás et al. (2014) when comparing well-watered and drought-stressed grapevine cultivars. Our results discard the influence of main leaf anatomical determinants of CO_2 diffusion on fast changes of g_m. Discarding the anatomy as a source for short-term g_m variation, this variation should reflect model weaknesses in the g_m estimation and/or the influence of biochemical factors like aquaporins and carbonic anhydrase.

In recent years, several reports have debated model weaknesses on g_m estimates. Gu and Sun (2014) proposed that a source of error comes from wrong parameterization of the chlorophyll fluorescence model. This source of error can be roughly solved by taking certain precautions. Specially, they suggest the use of an in-vitro based estimate of Γ* (Walker et al. 2013) instead of using the Laisk method (Laisk et al. 1984), in addition to get reliable R_d values as input (Galmés et al. 2011, Niinemets et al. 2005, Tosens et al. 2016). Gu and Sun (2014) also exposed that a source of error comes from the obligatory relationship between input parameters and g_m. This is very difficult to avoid, but a sensitivity analysis was performed to show that in most cases the observed responses of g_m were maintained even when using different parameterizations for R_d, Γ*, *A*, C_i, ETR or (*p1*,*p2*). Light variations were the most sensitive to parameter variations (not significant in 5 out of 12 cases), with the most influent being ETR, C_i and (*p*1, *p*2). CO_2 variations (especially high CO_2 effect) were the most robust, conserved 11 out of 12 times (Fig. S3). Recently, Xiong et al. (2015) also performed a careful sensitivity analysis of their data, showing a strong conservation of the patterns for the response to C_i. In this sense, although it is not possible to definitively discard the possibility of an artifact during g_m calculation, at least the apparent g_m response may not be due to a mathematical artifact from the fluorescence method only.

In addition to arising from mathematical artifacts, fluorescence and stable isotope models weaknesses have been suggested to be related with wrong modelling of the decarboxylation fluxes and their possible recycling (Tholen and Zhu 2011, Xiao and Zhu 2017) and from ignoring light gradients through the leaf mesophyll, both aspects potentially causing underestimation of the real g_m values (Evans et al. 2009, Théroux-Rancourt and Gilbert 2017). Both arguments describe problems that occur when the model used is too simplified, particularly with regard to: the recycling of CO_2, the balance between carboxylation and decarboxylation, and the positioning of chloroplasts and mitochondria, first pointed-out by Tholen and Zhu (2011) and further deeply described by Yin and Struik (2017) and Xiao and Zhu (2017). Parameters like the importance of chloroplast membrane conductance in respect to the total mesophyll conductance and mitochondria positioning are needed in order to estimate the importance of the recycling, and then be able to built-up a model representative of the true g_m (Xiao and Zhu 2017, Yin and Struik 2017). Also, Théroux-Rancourt and Gilbert (2017) have identified the light absorption across the leaf profile as a parameter ignored when measuring gas exchange (and leaf chlorophyll fluorescence). They conclude that highly saturating light conditions are needed to get a relatively equal contribution of all mesophyll cell layers to the total leaf apparent g_m allowing the determination of g_m variations. The only way to deal with g_m model limitations may be the use complex of modelling (3D structure, leaf ray tracing model, etc.) that needs not easy to measure parameters such as positioning of mitochondria, “real” resistance of the chloroplast envelop, or leakage of CA at the chloroplast envelop (Xiao and Zhu 2017, Yin and Struik 2017). The fact that a constant g_m can be modelled and can fit with observed data of assimilation rate cannot certify that g_m

is truly constant. The real nature of g_m will be revealed by a combination of strong modelling and direct measurements that fit/support the different models used, but a purely theoretical approach may not be sufficient.

Even considering the above-mentioned arguments, it can still be hypothesized that at least a part of the variations found by gas exchange are reflecting a true or partially true biological process. Thus, if leaf anatomy does not vary with [CO_2] nor light, this would mean that other factors are influencing leaf CO_2 diffusion properties in the short term. Aquaporins as trans-membrane proteins are likely to partially assume this role. Terashima and Ono (2002) and Uehlein et al. (2003) were pioneers in the idea that aquaporins, at that time already known to be involved in water transport in plants, could have the same role for trans-membrane CO_2 transport. Experiments using oocytes, transgenic plants with different expression of aquaporins and/or aquaporin inhibitors reinforced this hypothesis (Flexas et al. 2006, Maurel et al. 2008, Terashima and Ono 2002, Uehlein et al. 2003). Moreover, aquaporins seem to have some gating properties, the opening and closing of the pore (Maurel et al. 2008), that would change their diffusion capacity in the short term. Cochard et al. (2007) nicely showed how aquaporins in walnut tree are very likely to modulate the measured leaf hydraulic conductance at the minute scale. Since such mechanisms are apparently acting on water fluxes, the equivalent effects on CO_2 diffusion are highly probable too. Nevertheless, they would not be able to explain short-term g_m variations alone, as revealed by the model fitting (Fig. 3C, D). Other proteins probably involved in the facilitation of CO_2 diffusion inside the leaf has been identified, like carbonic anhydrase (Momayyezi and Guy 2017, Terashima et al. 2011). Their role consists to catalyse the CO_2/HCO_3^- conversion in the cytosol. Indeed, carbon diffuses much faster in liquid phase when it is in the HCO_3^- form. This finally improves CO_2 diffusion in the liquid phase (Terashima et al. 2011). Nevertheless, carbonic anhydrase is thought to be at sufficient concentration in the stroma, thus not being a limiting or varying factor in the short-term. Recent studies estimating g_m from anatomical factors choose not to incorporate this factor in the anatomical model (Peguero-Pina et al. 2017, Tosens et al. 2012).

Conclusions

The present study shows that the apparent mesophyll conductance estimated from gas exchange coupled to leaf chlorophyll fluorescence varied with C_i and light, as previously described in the literature. Different simulations considering varying model inputs were performed to check whether differences were maintained, and g_m changes under C_i variations appeared to be more conserved than those induced by light variations. While g_m does vary in the short-term in tobacco as determined with the chlorophyll fluorescence method, no change in any anatomical parameter was observed. This causes the absence of significant correlation between g_m values obtained by both fluorescence and two analytical models based on anatomical parameters. Moreover, theoretical modelling suggests not significant effect of aquaporins and (photo)respired CO_2 recycling due to the relative position of mitochondria and chloroplast on the dynamic response of g_m. Although more precise models and/or faster direct measurement methods are needed to refuse it, this work reinforces the idea that short-term variations of g_m at least partially reflect some artifactual rather than a biological effect.

Author contributions

M.C., C.D. and J.F. designed the study; M.C., C.D. and A.M. conducted the experiments; M.C., C.D. and J.F. performed the analysis and wrote the manuscript.

Acknowledgements – This work was supported by the Conselleria d'Educació, Cultura i Universitats (Govern de les Illes Balears) and European Social Fund, predoctoral fellowship FPI/1700/2014, awarded to MC. The authors are grateful to Miquel Ribas-Carbó for correction of the written English in the manuscript, to Javier Cano, for his helpful comments, to Miquel Truyols for his support to our experiment, and to Mª Teresa Mínguez, Universitat de València (Secció Microscòpia Electrònica, SCSIE), and Dr Ferran Hierro, Universitat de les Illes Balears (Serveis Cientificotècnics), for technical support during microscopic analyses. This work was supported by the project CTM2014-53902-C2-1-P from the Ministerio de Economía y Competitividad (MINECO, Spain) and the ERDF (FEDER).

References

Brodersen CR, Vogelmann TC (2010) Do changes in light direction affect absorption profiles in leaves? Funct Plant Biol 37: 403–412

von Caemmerer S, Evans JR (2015) Temperature responses of mesophyll conductance differ greatly between species. Plant Cell Environ 38: 629–637

Cochard H, Venisse J-S, Barigah TS, Brunel N, Herbette S, Guilliot A, Tyree MT, Sakr S (2007) Putative role of aquaporins in variable hydraulic conductance of leaves in response to light. Plant Physiol 143: 122–133

Douthe C, Dreyer E, Brendel O, Warren CR (2012) Is mesophyll conductance to CO_2 in leaves of three Eucalyptus species sensitive to short-term changes of irradiance under ambient as well as low O_2? Funct Plant Biol 39: 435–448

Douthe C, Dreyer E, Epron D, Warren CR (2011) Mesophyll conductance to CO_2, assessed from online TDL-AS records of $^{13}CO_2$ discrimination, displays small but significant short-term responses to CO_2 and irradiance in *Eucalyptus* seedlings. J Exp Bot 62: 5335–5346

Evans J, Caemmerer S, Setchell B, Hudson G (1994) The relationship between CO_2 transfer conductance and leaf anatomy in transgenic tobacco with a reduced content of Rubisco. Aust J Plant Physiol 21: 475–495

Evans JR (1989) Photosynthesis and nitrogen relationship in leaves of C_3 plants. Oecologia 78: 9–19

Evans JR (2009) Potential errors in electron transport rates calculated from chlorophyll fluorescence as revealed by a multilayer leaf model. Plant Cell Physiol 50: 698–706

Evans JR, Kaldenhoff R, Genty B, Terashima I (2009) Resistances along the CO_2 diffusion pathway inside leaves. J Exp Bot 60: 2235–48

Evans JR, Vogelmann TC (2003) Profiles of ^{14}C fixation through spinach leaves in relation to light absorption and photosynthetic capacity. Plant Cell Environ 26: 547–560

Flexas J, Barbour MM, Brendel O, Cabrera HM, Carriquí M, Díaz-Espejo A, Douthe C, Dreyer E, Ferrio JP, Gago J, Gallé A, Galmés J, Kodama N, Medrano H, Niinemets Ü, Peguero-Pina JJ, Pou A, Ribas-Carbó M, Tomás M, Tosens T, Warren CR (2012) Mesophyll diffusion conductance to CO_2: An unappreciated central player in photosynthesis. Plant Sci 193–194: 70–84

Flexas J, Diaz-Espejo A (2015) Interspecific differences in temperature response of mesophyll conductance: food for thought on its regulation. Plant Cell Environ 38: 625–628

Flexas J, Díaz-Espejo A, Berry JA, Cifre J, Galmés J, Kaldenhoff R, Medrano H, Ribas-Carbó M (2007a) Analysis of leakage in IRGA's leaf chambers of open gas exchange systems: Quantification and its effects in photosynthesis parameterization. J Exp Bot 58: 1533–1543

Flexas J, Diaz-Espejo A, Galmés J, Kaldenhoff R, Medrano H, Ribas-Carbo M (2007b) Rapid variations of mesophyll conductance in response to changes in CO_2 concentration around leaves. Plant Cell Environ 30: 1284–98

Flexas J, Ribas-Carbó M, Diaz-Espejo A, Galmés J, Medrano H (2008) Mesophyll conductance to CO_2: current knowledge and future prospects. Plant Cell Environ 31: 602–21

Flexas J, Ribas-Carbó M, Hanson DT, Bota J, Otto B, Cifre J, McDowell N, Medrano H, Kaldenhoff R (2006) Tobacco aquaporin NtAQP1 is involved in mesophyll conductance to CO_2 in vivo. Plant J 48: 427–39

Galle A, Florez-Sarasa I, Tomas M, Pou A, Medrano H, Ribas-Carbo M, Flexas J (2009) The role of mesophyll conductance during water stress and recovery in tobacco (*Nicotiana sylvestris*): acclimation or limitation? J Exp Bot 60: 2379–90

Galmés J, Conesa MÀ, Ochogavía JM, Perdomo JA, Francis DM, Ribas-Carbó M, Savé R, Flexas J, Medrano H, Cifre J (2011) Physiological and morphological adaptations in relation to water use efficiency in Mediterranean accessions of *Solanum lycopersicum*. Plant Cell Environ 34: 245–60

Galmés J, Medrano H, Flexas J (2006) Acclimation of Rubisco specificity factor to drought in tobacco: discrepancies between in vitro and in vivo estimations. J Exp Bot 57: 3659–67

Genty B, Briantais J-M, Baker NR (1989) The relationship between the quantum yield of photosynthetic electron transport and quenching of chlorophyll fluorescence. Biochim Biophys Acta - Gen Subj 990: 87–92

Griffiths H, Helliker BR (2013) Mesophyll conductance: Internal insights of leaf carbon exchange. Plant Cell Environ 36: 733–735

Gu L, Sun Y (2014) Artefactual responses of mesophyll conductance to CO_2 and irradiance estimated with the variable *J* and online isotope discrimination methods. Plant Cell Environ 37: 1231–49

Harley PC, Loreto F, Di Marco G, Sharkey TD (1992) Theoretical considerations when estimating the mesophyll conductance to CO_2 flux by analysis of the response of photosynthesis to CO_2. Plant Physiol 98: 1429–36

Hassiotou F, Ludwig M, Renton M, Veneklaas EJ, Evans JR (2009) Influence of leaf dry mass per area, CO_2, and irradiance on mesophyll conductance in sclerophylls. J Exp Bot 60: 2303–2314

Heinen RB, Ye Q, Chaumont F (2009) Role of aquaporins in leaf physiology. J Exp Bot 60: 2971–2985

Higa T, Wada M (2016) Chloroplast avoidance movement is not functional in plants grown under strong sunlight. Plant Cell Environ 39: 871–882

Ho QT, Berghuijs HNC, Watté R, Verboven P, Herremans E, Yin X, Retta MA, Aernouts B, Saeys W, Helfen L, Farquhar GD, Struik PC, Nicolaï BM (2016) Three-dimensional microscale modelling of CO_2 transport and light propagation in tomato leaves enlightens photosynthesis. Plant Cell Environ 39: 50–61

Kasahara M, Kagawa T, Oikawa K, Suetsugu N, Miyao M, Wada M (2002) Chloroplast avoidance movement reduces photodamage in plants. Nature 420: 829–832

Laisk A, Kiirats O, Oja V (1984) Assimilatory power (postillumination CO_2 uptake) in leaves: measurement, environmental dependencies, and kinetic properties. Plant Physiol 76: 723–729

Lloyd J, Syvertsen JP, Kriedemann PE, Farquhar GD (1992) Low conductances for CO_2 diffusion from stomata to the sites of carboxylation in leaves of woody species. Plant Cell Environ 15: 873–899

Martins SCV, Galmés J, Molins A, DaMatta FM (2013) Improving the estimation of mesophyll conductance to CO2: on the role of electron transport rate correction and respiration. J Exp Bot 64: 3285-3298

Maurel C, Verdoucq L, Luu D-T, Santoni V (2008) Plant aquaporins: membrane channels with multiple integrated functions. Annu Rev Plant Biol 59: 595–624

Mendiburu F (2015). agricolae: Statistical Procedures for Agricultural Research. R package version 1:2-3. https://CRAN.R-project.org/package=agricolae)

Momayyezi M, Guy RD (2017) Substantial role for carbonic anhydrase in latitudinal variation in mesophyll conductance of *Populus trichocarpa* Torr. & Gray. Plant, Cell Environ 40: 138-149

Niinemets Ü, Cescatti A, Rodeghiero M, Tosens T (2005) Leaf internal diffusion conductance limits photosynthesis more strongly in older leaves of Mediterranean evergreen broad-leaved species. Plant, Cell Environ 28: 1552–1566

Niinemets Ü, Reichstein M (2003) Controls on the emission of plant volatiles through stomata: Differential sensitivity of emission rates to stomatal closure explained. J Geophys Res 108: 4208

Oguchi R, Hikosaka K, Hirose T (2005) Leaf anatomy as a constraint for photosynthetic acclimation: Differential responses in leaf anatomy to increasing growth irradiance among three deciduous trees. Plant, Cell Environ 28: 916–927

Peguero-Pina JJ, Flexas J, Galmés J, Niinemets U, Sancho-Knapik D, Barredo G, Villarroya D, Gil-Pelegrín E (2012) Leaf anatomical properties in relation to differences in mesophyll conductance to CO_2 and photosynthesis in two related Mediterranean *Abies* species. Plant Cell Environ 35: 2121–9

Peguero-Pina JJ, Sisó S, Flexas J, Galmés J, García-Nogales A, Niinemets Ü, Sancho-Knapik D, Saz MÁ, Gil-Pelegrín E (2017) Cell-level anatomical characteristics explain high mesophyll conductance and photosynthetic capacity in sclerophyllous Mediterranean oaks. New Phytol 214: 585–596

Perez-Martin A, Michelazzo C, Torres-Ruiz JM, Flexas J, Fernandez JE, Sebastiani L, Diaz-Espejo A (2014) Regulation of photosynthesis and stomatal and mesophyll conductance under water stress and recovery in olive trees: correlation with gene expression of carbonic anhydrase and aquaporins. J Exp Bot 65: 3143–3156

Poorter H, Niinemets Ü, Poorter L, Wright IJ, Villar R, Niinemets U, Poorter L, Wright IJ, Villar R (2009) Causes and consequences of variation in leaf mass per area (LMA):a meta-analysis. New Phytol 182: 565–588

R Core Team (2016). R: A language and environment for statistical computing. R Foundation for Statistical Computing, Vienna, Austria. URL https://www.R-project.org/)

Rondeau-Mouro C, Defer D, Leboeuf E, Lahaye M (2008) Assessment of cell wall porosity in *Arabidopsis thaliana* by NMR spectroscopy. Int J Biol Macromol 42: 83–92

Schneider CA, Rasband WS, Eliceiri KW (2012) "NIH Image to ImageJ: 25 years of image analysis". Nature methods 9: 671-675

Syvertsen JP, Lloyd J, McConchie C, Kriedemann PE, Farquhar GD (1995) On the relationship between leaf anatomy and CO_2 diffusion through the mesophyll of hypostomatous leaves. Plant Cell Environ 18: 149–157

Tazoe Y, Von Caemmerer S, Badger MR, Evans JR (2009) Light and CO_2 do not affect the mesophyll conductance to CO_2 diffusion in wheat leaves. J Exp Bot 60: 2291–2301

Terashima I, Hanba YT, Tholen D, Niinemets Ü (2011) Leaf functional anatomy in relation to photosynthesis. Plant Physiol 155: 108–116

Terashima I, Ono K (2002) Effects of $HgCl_2$ on CO_2 dependence of leaf photosynthesis: evidence indicating involvement of aquaporins in CO_2 diffusion across the plasma membrane. Plant Cell Physiol 43: 70–78

Terashima I, Saeki T (1985) A new model for leaf photosynthesis incorporating the gradients of light environment and of photosynthetic properties of chloroplasts within a leaf. Ann Bot 56: 489–499

Thain JF (1983) Curvature correlation factors in the measurements of cell surface areas in plant tissues. J Exp Bot 34: 87-94

Théroux-Rancourt G, Gilbert ME (2017) The light response of mesophyll conductance is controlled by structure across leaf profiles. Plant Cell Environ 40: 726–740

Tholen D, Boom C, Noguchi K, Ueda S, Katase T, Terashima I (2008) The chloroplast avoidance response decreases internal conductance to CO_2 diffusion in *Arabidopsis thaliana* leaves. Plant Cell Environ 31: 1688–1700

Tholen D, Zhu X-G (2011) The Mechanistic Basis of Internal Conductance: A theoretical analysis of mesophyll cell photosynthesis and CO_2 diffusion. Plant Physiol 156: 90–105

Tomás M, Flexas J, Copolovici L, Galmés J, Hallik L, Medrano H, Ribas-Carbó M, Tosens T, Vislap V, Niinemets Ü (2013) Importance of leaf anatomy in determining mesophyll diffusion conductance to CO_2 across species: quantitative limitations and scaling up by models. J Exp Bot 64: 2269–2281

Tomás M, Medrano H, Brugnoli E, Escalona JM, Martorell S, Pou A, Ribas-Carbó M, Flexas J (2014) Variability of mesophyll conductance in grapevine cultivars under water stress conditions in relation to leaf anatomy and water use efficiency. Aust J Grape Wine Res 20: 272–280

Tosens T, Niinemets U, Vislap V, Eichelmann H, Castro Díez P (2012a) Developmental changes in mesophyll diffusion conductance and photosynthetic capacity under different light and water availabilities in *Populus tremula*: how structure constrains function. Plant Cell Environ 35: 839–56

Tosens T, Niinemets Ü, Westoby M, Wright IJ (2012b) Anatomical basis of variation in mesophyll resistance in eastern Australian sclerophylls: news of a long and winding path. J Exp Bot 63: 5105–5119

Tosens T, Nishida K, Gago J, Coopman RE, Cabrera HM, Carriquí M, Laanisto L, Morales L, Nadal M, Rojas R, Talts E, Tomas M, Hanba Y, Niinemets Ü, Flexas J (2016) The photosynthetic capacity in 35 ferns and fern allies: Mesophyll CO_2 diffusion as a key trait. New Phytol 209: 1576–1590

Trojan A, Gabrys H (1996) Chloroplast distribution in *Arabidopsis thaliana* (L.) depends on light conditions during growth. Plant Physiol 111: 419–425

Uehlein N, Lovisolo C, Siefritz F, Kaldenhoff R (2003) The tobacco aquaporin NtAQP1 is a membrane CO_2 pore with physiological functions. Nature 425: 734–737

Uehlein N, Otto B, Hanson DT, Fischer M, McDowell N, Kaldenhoff R (2008) Function of *Nicotiana tabacum* aquaporins as chloroplast gas pores challenges the concept of membrane CO_2 permeability. Plant Cell 20: 648–57

Valentini R, Epron D, Deangelis P, Matteucci G, Dreyer E (1995) In-situ estimation of net CO_2 assimilation, photosynthetic electron flow and photorespiration in Turkey oak (*Q.cerri*s L.) leaves: diurnal cycles under different levels of water supply. Plant Cell Environ 18: 631–640

Veromann-Jürgenson L-L, Tosens T, Laanisto L, Niinemets Ü (2017) Extremely thick cell walls and low mesophyll conductance: welcome to the world of ancient living! J Exp Bot 68: 1639–1653

Vogelmann TC, Bornman JF, Josserand S (1989) Photosynthetic light gradients and spectral regime within leaves of *Medicago sativa*. Philos Trans R Soc B Biol Sci 323: 411–421

Walker B, Ariza LS, Kaines S, Badger MR, Cousins AB (2013) Temperature response of in vivo Rubisco kinetics and mesophyll conductance in Arabidopsis thaliana: comparisons to *Nicotiana tabacum*. Plant Cell Environ 36: 2108–19

Weisiger R (1998) Impact of extracellular and intracellular diffusion barriers on transport. In J Bassingthwaighte, C Goresky, J Linehan, eds, Whole organ approach to Cell. Metab. Springer-Verlag, New York, NY, US, p 389.423

Xiao Y, Zhu X-G (2017) Components of mesophyll resistance and their environmental responses a theoretical modeling analysis. Plant Cell Environ. doi: 10.1111/pce.13040

Xiong D, Liu X, Liu L, Douthe C, Li Y, Peng S, Huang J (2015) Rapid responses of mesophyll conductance to changes of CO_2 concentration, temperature and irradiance are affected by N supplements in rice. Plant Cell Environ 12: 2541–2550

Yamori W, Noguchi K, Hanba YT, Terashima I (2006) Effects of internal conductance on the temperature dependence of the photosynthetic rate in spinach leaves from contrasting growth temperatures. Plant Cell Physiol 47: 1069–1080

Yin X, Struik PC (2017) Simple generalisation of a mesophyll resistance model for various intracellular arrangements of chloroplasts and mitochondria in C_3 leaves. Photosynth Res 132: 211–220

Yin X, Struik PC, Romero P, Harbinson J, Evers JB, Van Der Putten PEL, Vos J (2009) Using combined measurements of gas exchange and chlorophyll fluorescence to estimate parameters of a biochemical C_3 photosynthesis model: A critical appraisal and a new integrated approach applied to leaves in a wheat (*Triticum aestivum*) canopy. Plant Cell Environ 32: 448–464

Fig. 1. Box plots of net CO_2 assimilation rate (*A*), stomatal conductance (g_s) and mesophyll conductance (g_m) for each low light (LL; 200 µmol photons m^{-2} s^{-1}), medium light (ML; 600 µmol photons m^{-2} s^{-1}) and high light (HL; 1500 µmol photons m^{-2} s^{-1}) treatment. The two extreme lines of the boxplot (*whiskers*) show the 10 and 90% percentiles, the two bounds of the box the 25 and 75% percentiles, and the center thick line the median. Dots represent data out of the shown percentiles. Leaf inside the Li-6400 photosynthesis chamber was kept at least 15 minutes in the given environmental condition. Letters indicate significant differences following Tukey's Post-Hoc test, at $P < 0.05$. n = 6-7.

Fig. 2. Box plots of net CO_2 assimilation rate (*A*), stomatal conductance (g_s) and mesophyll conductance (g_m) for each low CO_2 (LCO_2; 100 ppm CO_2), medium CO_2 (MCO_2; 400 ppm CO_2) and high CO_2 (HCO_2; 1500 ppm) treatment. The two extreme lines of the boxplot (*whiskers*) show the 10 and 90% percentiles, the two bounds of the box the 25 and 75% percentiles, and the center thick line the median. Dots represent data out of the shown percentiles. Leaf inside the Li-6400 photosynthesis chamber was kept at least 15minutes in the given environmental condition. Letters indicate significant differences following Tukey's Post-Hoc test, at $P < 0.05$. n = 6-8, except for g_m under 100 ppm (n = 1) and 1500 ppm (n = 2) after filtering for Harley's criteria. All the g_m data (not filtered for Harley's criteria) are presented in Fig. S1.

Fig. 3. Comparison of g_m calculated based on Harley et al. (1992) with g_m modelled from anatomy estimated according to the diffusion model from Tosens et al. (2012, 2016). In (A) closed circles represent the estimated g_m from anatomy, while open circles are simulated g_m anatomy using a variable fitted chloroplast surface area exposed to intercellular airspaces (S_c/S); in (B) the observed S_c/S (closed circles) and the required S_c/S to match g_m anatomy to g_m Harley (open circles) are represented; in (C) closed circles represent the estimated g_m from anatomy, while open circles are simulated g_m anatomy using a variable fitted plasma membrane conductance (g_{pl}); in (D) the assumed g_{pl} (closed circles) and the required g_{pl} to match g_m anatomy to g_m Harley (open circles) are represented. Each point corresponds to an individual replicated plant for the five combinations of CO_2 and light treatments.

Fig. 4. Comparison of mesophyll conductance calculated from analytical models of Xiao and Zhu (2017; open circles) and Tomás et al. (2013; closed circles) in relation to mesophyll conductance calculated based on Harley et al. (1992). Grey dashed line represents 1:1 correlation.

Supporting information

Additional supporting information may be found in the online version of this article:

Fig. S1. g_m under CO_2 variation not filtered for the Harley's criteria.

Fig. S2. Light and CO_2 response curves for *A* and g_m.

Fig. S3. Sensitivity analysis of the dataset.

Fig. S4. Comparison of g_m estimated from Harley et al. (1992) and Yin et al. (2009) methods.

Fig. S5. Micrograph cross-sections for each CO_2 and light treatments.

Fig. S6. Bootstrap percentages for chloroplast significant differences.

Fig. S7. Sensitivity analysis of the (photo)respired CO_2 effect on g_m.

Methods S1. Calculation of variables used for unit conversion using the Xiao and Zhu (2017) model

Table 1. Light and CO_2 conditions in the photosynthesis chamber of the Li-6400 for each treatment applied.

Treatment	$[CO_2]$ entering the chamber (μmol mol^{-1})	PPFD (μmol photons m^{-2} s^{-1})
LCO_2	100	1500
MCO_2/HL	400	1500
HCO_2	1500	1500
LL	400	200
ML	400	600

Table 2. Leaf thickness (T_{leaf}), total mesophyll thickness (T_{mes}), number of palisade layers, fraction of the mesophyll occupied by the intercellular air spaces (f_{ias}), mesophyll surface area exposed to intercellular airspace (S_m/S), chloroplast surface area exposed to intercellular airspace (S_c/S), the ratio S_c/S_m, mesophyll cell wall thickness (T_{cw}), cytoplasm thickness (T_{cyt}), chloroplast length (L_{chl}), chloroplast thickness (T_{chl}) and mesophyll conductance to CO_2 modelled by anatomy (g_m anatomy) in tobacco leaves subjected to a short-term 100 ppm (LCO_2), 400 ppm (MCO_2) and 1500 ppm (HCO_2) CO_2 treatment. Data are mean ± SE (n = 4-6). Different letters indicate statistically significant differences ($P < 0.05$) between treatments. In bold the only significant change observed between treatments.

Parameters	***LCO_2***	***MCO_2***	***HCO_2***
T_{leaf} (μm)	211 ± 8^a	205 ± 8^a	206 ± 12^a
T_{mes} (μm)	172 ± 7^a	170 ± 6^a	170 ± 9^a
Number of palisade layers	1.25	1.05	1.10
f_{ias}	0.41 ± 0.01^a	0.43 ± 0.01^a	0.43 ± 0.01^a
S_m/S (m^2 m^{-2})	10.4 ± 0.5^a	10.1 ± 0.8^a	11.4 ± 0.2^a
S_c/S (m^2 m^{-2})	7.7 ± 0.3^a	8.0 ± 0.7^a	9.1 ± 0.1^a
S_c/S_m	0.74 ± 0.03^a	0.81 ± 0.05^a	0.80 ± 0.00^a
T_{cw} (μm)	0.122 ± 0.012^a	0.128 ± 0.007^a	0.122 ± 0.003^a
T_{cyt} (μm)	0.28 ± 0.003^a	0.30 ± 0.02^a	0.38 ± 0.04^a
L_{chl} (μm)	5.05 ± 0.19^a	5.60 ± 0.22^a	5.26 ± 0.13^a
T_{chl} (μm)	**2.81 ± 0.06^a**	**3.44 ± 0.10^b**	**3.08 ± 0.17^{ab}**
g_m anatomy (mol m^{-2} s^{-1})	0.086 ± 0.005^a	0.078 ± 0.005^a	0.093 ± 0.005^a

Table 3. Leaf thickness (T_{leaf}), total mesophyll thickness (T_{mes}), number of palisade layers, fraction of the mesophyll occupied by the intercellular air spaces (f_{ias}), mesophyll surface area exposed to intercellular airspace (S_m/S), chloroplast surface area exposed to intercellular airspace (S_c/S), the ratio S_c/S_m, mesophyll cell wall thickness (T_{cw}), cytoplasm thickness (T_{cyt}), chloroplast length (L_{chl}), chloroplast thickness (T_{chl}) and mesophyll conductance to CO_2 modelled by anatomy (g_m anatomy) in tobacco leaves subjected to a short-term light treatment of 200 (LL), 600 (ML) or 1500 µmol m^{-2} s^{-1} (HL) light treatment. Data are mean ± SE (n = 4-6). Different letters indicate statistically significant differences (P < 0.05) between treatments. In bold the only significant change observed between treatments.

Parameters	***LL***	***ML***	***HL***
T_{leaf} (µm)	195 ± 6^{a}	200 ± 11^{a}	205 ± 8^{a}
T_{mes} (µm)	164 ± 6^{a}	165 ± 10^{a}	170 ± 6^{a}
Number of palisade layers	1.12	1.13	1.05
f_{ias}	0.42 ± 0.02^{a}	0.43 ± 0.02^{a}	0.43± 0.01^{a}
S_m/S (m^2 m^{-2})	11.0 ± 0.4^{a}	10.4 ± 0.5^{a}	10.1 ± 0.8^{a}
S_c/S (m^2 m^{-2})	8.3 ± 0.3^{a}	7.6 ± 0.6^{a}	8.0 ± 0.7^{a}
S_c/S_m	0.77 ± 0.03^{a}	0.73 ± 0.04^{a}	0.81 ± 0.05^{a}
T_{cw} (µm)	0.119 ± 0.008^{a}	0.108 ± 0.006^{a}	0.128 ± 0.007^{a}
T_{cyt} (µm)	0.27 ± 0.005^{a}	0.25 ± 0.02^{a}	0.30 ± 0.02^{a}
L_{chl} (µm)	**6.28 ± 0.13^{b}**	**5.70 ± 0.12^{ab}**	**5.60 ± 0.22^{a}**
T_{chl} (µm)	3.35 ± 0.08^{a}	3.28 ± 0.12^{a}	3.44 ± 0.10^{a}
g_m anatomy (mol m^{-2} s^{-1})	0.084 ± 0.005^{a}	0.081 ± 0.006^{a}	0.078 ± 0.005^{a}

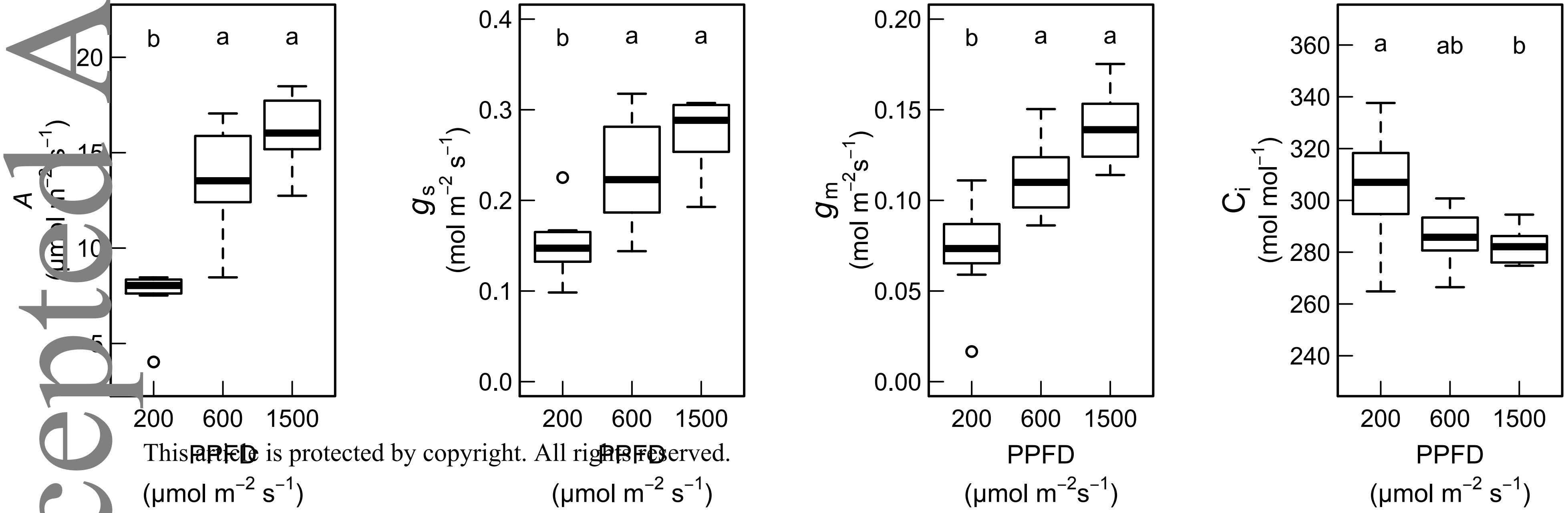

b
a
a
20
10
A
200
600
1500
PPFD
(μmol m^{-2} s^{-1})
0.4
0.3
0.2
0.1
0.0
b
a
a
g_s
(mol m^{-2} s^{-1})
200
600
1500
PPFD
(μmol m^{-2} s^{-1})
0.20
0.15
0.10
0.05
0.00
b
a
a
g_m
(mol m^{-2}s^{-1})
200
600
1500
PPFD
(μmol m^{-2}s^{-1})
360
340
320
300
280
260
240
a
ab
b
C_i
(mol mol^{-1})
200
600
1500
PPFD
(μmol m^{-2} s^{-1})

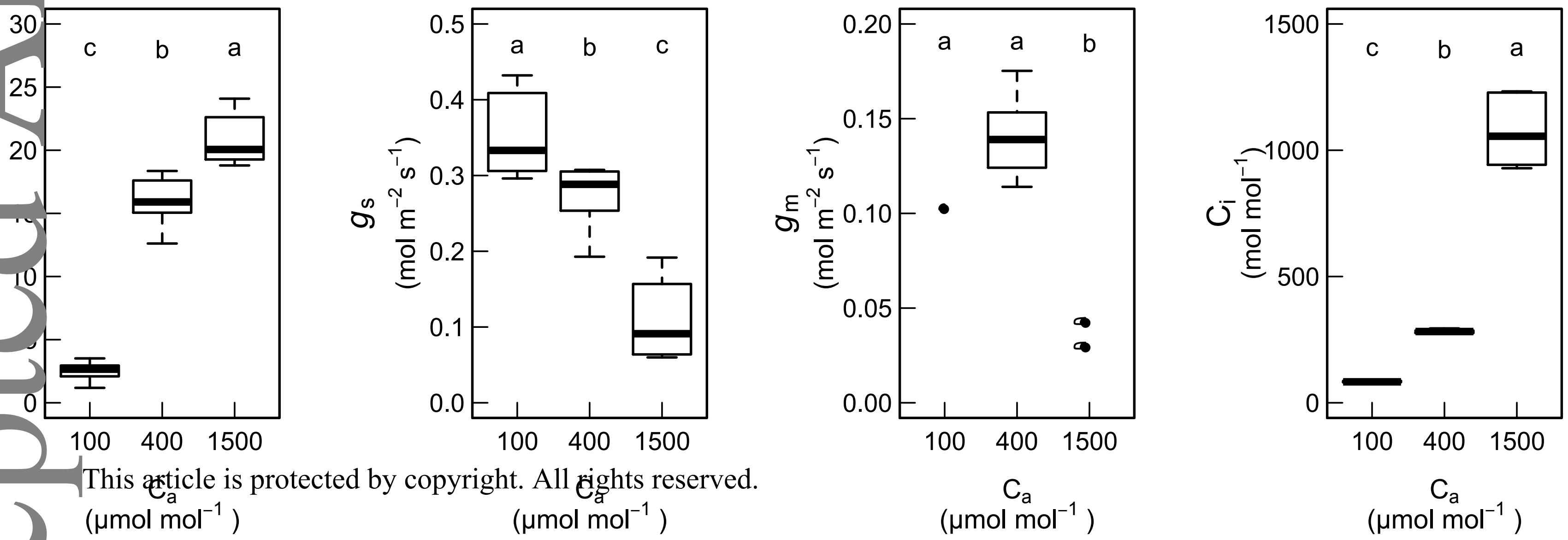
c
b
a
100
400
1500
C_a
(µmol mol^{-1})
a
b
c
g_s
(mol m^{-2} s^{-1})
0.0
0.1
0.2
0.3
0.4
0.5
100
400
1500
C_a
(µmol mol^{-1})
a
a
b
g_m
(mol m^{-2} s^{-1})
0.00
0.05
0.10
0.15
0.20
100
400
1500
C_a
(µmol mol^{-1})
c
b
a
C_i
(mol mol^{-1})
0
500
1000
1500
100
400
1500
C_a
(µmol mol^{-1})

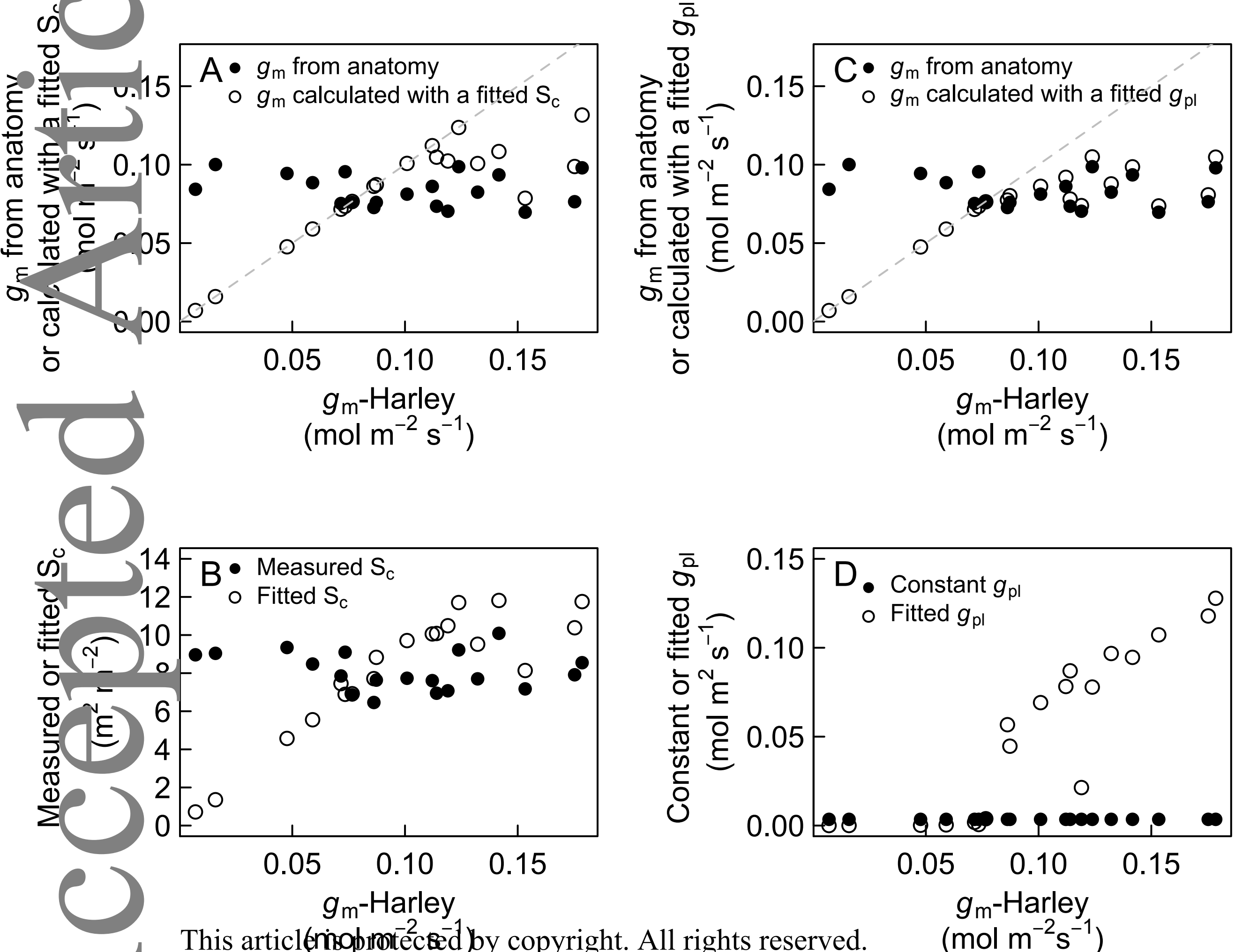

A
g_m from anatomy
g_m calculated with a fitted S_c
g_m from anatomy or calculated with a fitted S_c (mol m^{-2} s^{-1})
0.00
0.05
0.10
0.15
g_m-Harley (mol m^{-2} s^{-1})
C
g_m from anatomy
g_m calculated with a fitted g_{pl}
g_m from anatomy or calculated with a fitted g_{pl} (mol m^{-2} s^{-1})
B
Measured S_c
Fitted S_c
Measured or fitted S_c (m^2 m^{-2})
0
2
4
6
8
10
12
14
D
Constant g_{pl}
Fitted g_{pl}
Constant or fitted g_{pl} (mol m^2 s^{-1})
g_m-Harley (mol $m^{-2}$$s^{-1}$)

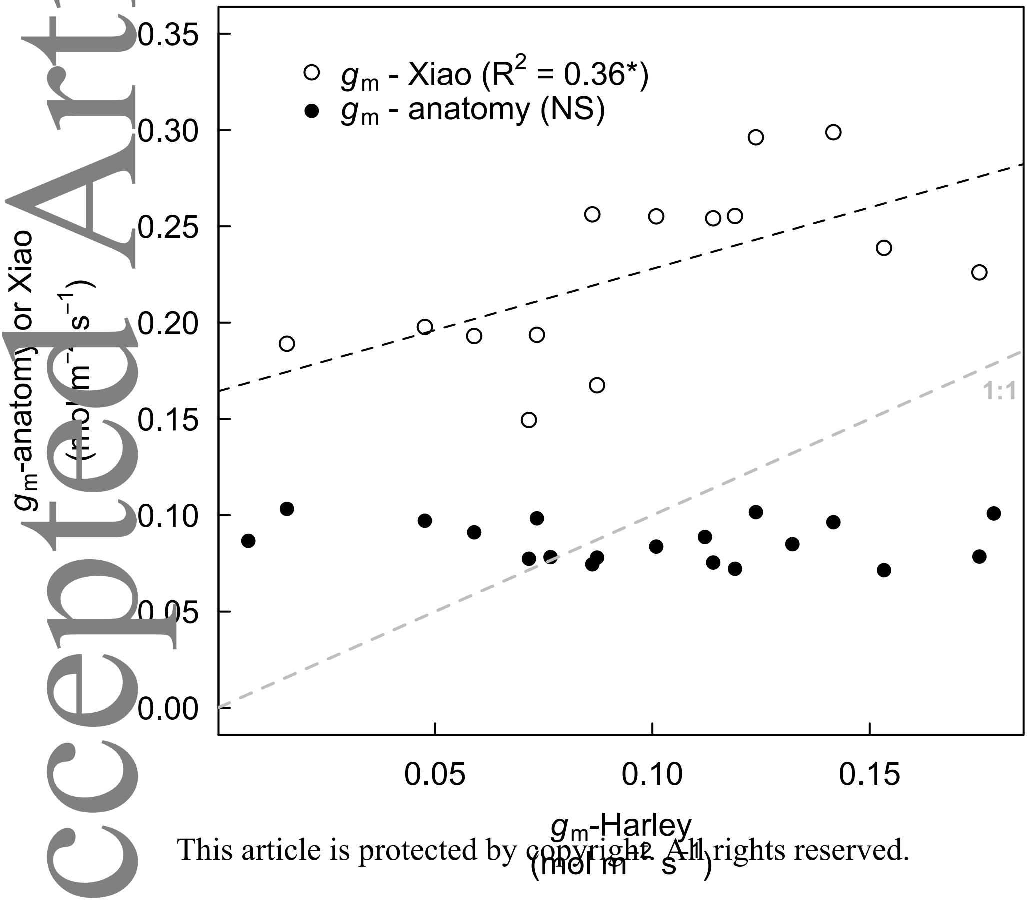
g_m - Xiao (R^2 = 0.36*)
g_m - anatomy (NS)
1:1
g_m-anatomy or Xiao (mol m^{-2} s^{-1})
0.35
0.30
0.25
0.20
0.15
0.10
0.05
0.00
0.05
0.10
0.15
g_m-Harley (mol m^{-2} s^{-1})